Diyala Journal of Engineering Sciences

Journal homepage: https://djes.info/index.php/djes

ISSN: 1999-8716 (Print); 2616-6909 (Online)

Evaluation of the Mechanical Properties of PLA Material Used For 3D Printing Solar E-Hub Component

Md. Helal Uddin[1,2*], Mohammad Nur-E-Alam[1,3,4], Abreeza Manap[1,2], Boon Kar Yap[1], and Md. Rokonuzzaman[1]

[1] Institute of Sustainable Energy (ISE), University Tenaga Nasional (UNITEN), Kajang 43000, Selangor, Malaysia
[2] Department of Mechanical Engineering, University of Tenaga Nasional, Jalan-Ikram, UNITEN, 43000, Kajang, Selangor, Malaysia
[3] School of Science, Edith Cowan University, 270 Joondalup Drive, Perth, Australia
[4] School of Engineering and Technology, Central Queensland University Australia, Melbourne, VIC 3000, Australia

ARTICLE INFO

Article history:
Received June 15, 2024
Revised August 24, 2024
Accepted August 29, 2024
Available online September 1, 2024

Keywords:
Additive manufacturing
Sustainable materials
Solar e-hub
Mechanical testing
Polylactic acid (PLA)

ABSTRACT

The advent of additive manufacturing (AM) technologies revolutionized design and production processes across various industries. In renewable energy, AM enabled new possibilities for optimizing solar e-hub (solar energy harvesting module) configurations, enhancing efficiency and performance. This study examined critical considerations such as material selection, durability, and cost-effectiveness in solar hub development. This fast-prototyping technique was controlled by computer-aided design (CAD) software like CREO Parametric 7.0 and Creality Slicer 4.8. Experimental results indicated that PLA (Polylactic acid) materials exhibited superior strength, with an impact energy of 4.8 Joules. The deformation study revealed that the maximum load of 22 MPa aligned with the ultimate tensile strength of PLA, and a hardness test result of 83.1 HRF featured its exemplary hardness properties. These findings advanced the understanding of using AM to investigate mechanical behaviours of PLA materials and optimize solar e-hub configurations for portable device applications, promoting sustainable energy solutions and the adoption of renewable energy technologies. In addition, the successful implementation of this approach will enable the renewable energy sectors to minimize the carbon foot-prints towards helping the global net-zero emissions by aligning the circular economy approach.

1. Introduction

In recent times, there has been a rising interest in additive manufacturing (AM) technologies, due to their ability to generate complex-shaped objects in a relatively short time [1]. AM, also recognized as 3D printing, presents a disruptive solution to these challenges by enabling the fabrication of intricate geometries, customized components, and lightweight structures with enhanced efficiency [2,3]. The Fused Deposition Method (FDM) technique, developed by Stratasys Inc., has gained global recognition as one of the finest prominent 3D printing techniques. In the FDM process, modules are constructed layer by layer, resulting in aeolotropic mechanical properties. Initially, raw materials are ejected into the nozzle, transforming from a filament to a semi-liquid state. Subsequently, the semi-liquid material is deposited on the above layer. During the 3D printing process, the material is cooled and solidified, integrating seamlessly with the surrounding materials. After each layer is deposited, the supporting platform lowers by one layer's height, allowing the next layer to be printed. Recent study shows the most used materials in FDM printers include

* Corresponding author.
E-mail address: mdhelaluddinarnob@gmail.com
DOI: 10.24237/djes.2024.17311

thermoplastics like PLA and ABS, as well as metal matrix composites, ceramic composites, and composites reinforced with natural fibers. Utilizing renewable energy sources for energy harvesting is a promising method to power such electrolysis processes [4-6]. The use of sustainable energy sources has prompted significant advancements in renewable [7,8] and portable energy technologies mostly empowering with solar energy considered as a prominent contender [9-11]. Solar hubs, comprising arrays of photovoltaic panels, play a pivotal role in harnessing solar energy efficiently [12]. However, the conventional manufacturing methods used for constructing these hubs often impose limitations on design flexibility, material selection, and cost-effectiveness. Approximately 3.5 billion people worldwide, mostly in impoverished off-grid areas [13,14] of developing nations do not have access to sustainable and reliable energy services. For these communities, there are options with variable renewable energies, mostly portable solar energy systems. The provision of affordable and clean energy for all is required by the seventh Sustainable Development Goal (SDG) [15-17]. Portable power sources are preferable but need application-specific advanced and compact device modules, including all solar component housing compartments [18]. Nonetheless, there are limitations in understanding the mechanical properties of 3D printing materials. In order to enhance the understanding and development of 3D printing structures, a recent study has focused on advancing the theoretical and practical examination of the ultimate tensile strength of FDM materials, specifically PLA. The investigations delved into variations in printing angles, materials, and printing techniques through both theoretical analysis and experimental studies. [19]. PLA, derived from renewable raw materials [20], boasts a reduced carbon footprint compared to fossil-based plastics for two main reasons: crops absorb CO_2 during growth, and the production of PLA requires less energy, resulting in fewer greenhouse gas emissions than fossil-based plastics [21]. PLA generally flows smoothly through a 3D printer's nozzle without clogging issues. Additionally, PLA has a relatively low print temperature and is cost-effective compared to other filaments. 3D printing represents a unique, innovative additive manufacturing technology that forms objects from digitized models deprived of the need for conventional, costly cutting or casting machines [22]. It accelerates in fabricating components with complex shapes and multi-material components, surpassing other methods [23]. Moreover, significant raw material savings are realized during the printing process. FDM is a 3D printing process used in this study which works by melting and extruding filament through a heated nozzle. FDM technology provides great printing quality with high precision for design electronics hosting modules [24]. The molten plastic is ejected through the nozzle and deposited on top of the previous layers, following the toolpath generated by the slicing software. The printer continues to deposit successive layers of melted filament, with each layer bonding to the previous one as it cools and solidifies. This process is repeated until the entire object is built up layer by layer. As each layer is deposited, it quickly cools and solidifies, forming a solid part [25].

This study sets the stage for exploring the potential of additive manufacturing in optimizing the configuration of solar e-hubs. It highlights the increasing demand for renewable energy solutions and the need for innovative approaches to enhance the performance and sustainability of solar power systems. It seeks to address key challenges such as material selection, structural integrity, and scalability inherent in the adoption of additive manufacturing for portable device casings.

2. Methodology

Figure 1 depicts the brief methods of the solar e-hub fabrication process. The methods begin with materials selection. PLA materials were used in this study. The CAD design of the different shapes was modeled using Creo Parametric version 7.0 CAD software. The designed file was converted into stereolithography file (stl) format and sliced using This fast-prototyping technique is

controlled by CAD software like CREO Parametric 7.0 and Creality Slicer 4.8. software. The file was later imported to a 3D printer for fabrication. Solar modules are integrated into the hub based on specific applications. Mechanical characterizations were performed to understand the material behaviors and properties.

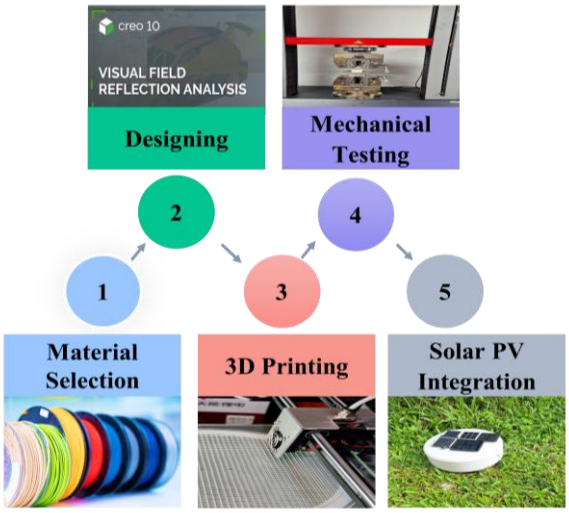

Figure 1. The fabrication and characterization methods of solar e-hub

2.1 Designing of CAD model

Figure 2 shows the designing steps of solar e-hub. The Creo Parametric 7.0 was used for CAD modelling. The modelling starts with choosing the standard template mmns_part_solid_abs (millimeter newton second with absolute) accuracy extension for the designs. Right datum plan was chosen to start the sketching. The surface sketch was designed on the right plane as a standard plane to create 2D object. There were use of centerline and reference line to make the drawing precise. Then inserting the proper dimension in millimeter and was extruded to 3D object. Utilizing additional features such as chamfer and to refine geometry and avoid sharp edges. Ensuring all the features and dimensions were accurate. Finally, completed the modelling for the ultimate view of the 3D model. The designed file was converted into STL file which is the most universal in 3D printing technology due to accuracy in 3D fabrication.

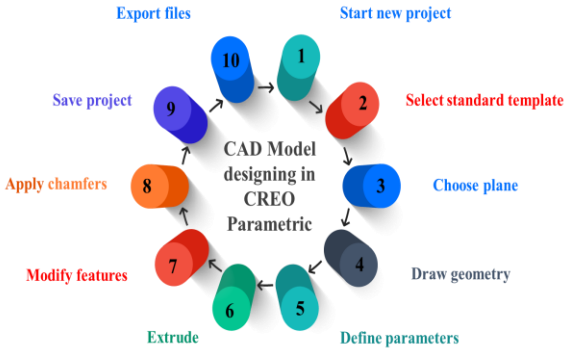

Figure 2. CAD model designing phases

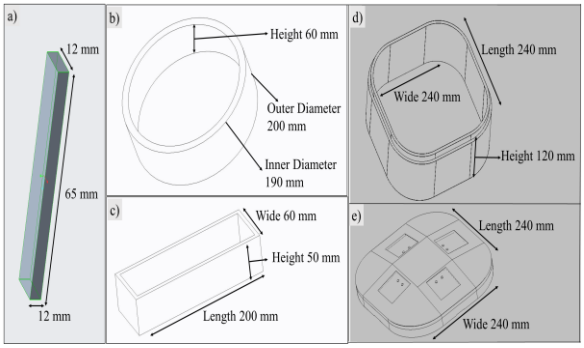

Figure 3. CAD model designing using CREO Parametric

The mechanical testing samples, as presented in Figure 3(a), is designed to undergo a series of rigorous assessments to investigate its mechanical properties. The samples will first be employed for impact test, hardness test and compression test respectively. Three different solar e-hub models were designed for 1-Watt applications, each solar e-hub's has unique geometries and functionalities. Figures 3(b) show a circular e-hub with solar cells mounted on the top surface and internal circuitry housed within, featuring a protective lid with openings for a USB slot and power switch. A rectangular e-hub shows in Figures 3(c) with solar cells on the upper surface and internal circuitry enclosed, including a rectangular cutout on the right side for a USB port. The Figure 3(d-e) shows a rounded cuboid e-hub designed to accommodate breadboard circuits, sensors, and other electrical components, with a specially crafted lid for solar cells and a 45-degree angle for optimal solar performance, accenting both functionality and versatility.

2.2 3D printing of ehubs

Figure 4 shows the 3D printing methods for fabrication. Creality Slicer 4.8 software is used for slicing the model and meshing. Before starting the fabrication process the amount of filament needs to be checked carefully to have smooth continuous printing. Applying glue on the printing bed is a good practice that helps to securely hold the printed model in its correct position and facilitates the effortless removal of objects. Different materials have different printing temperatures, however for PLA materials 70^0 C was found optimal for removing from printing bed.

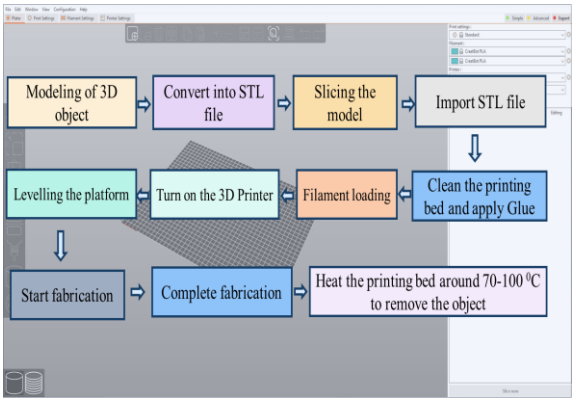

Figure 4. FDM fabrication process

3. FDM Fabrication Process

FDM is a 3D printing process used in this study which works by melting and extruding filament through a heated nozzle. FDM technology provides great printing quality with high precision for design electronics hosting modules [26]. The molten plastic is ejected through the nozzle and deposited on top of the previous layers, following the toolpath generated by the slicing software. The printer continues to deposit successive layers of melted filament, with each layer bonding to the previous one as it cools and solidifies. This process is repeated until the entire object is built up layer by layer. As each layer is deposited, it quickly cools and solidifies, forming a solid part [27]. The Figure 5(a) depicts the fabrication process and Figure 5(b) shows the picture of 3D printer.

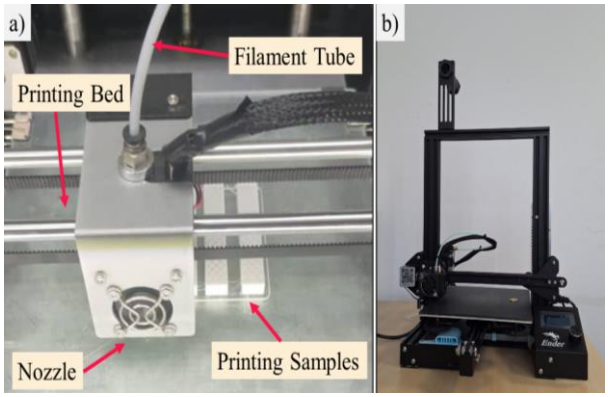

Figure 5. a) The fabrication process of solar ehub and b) Creality Ender V 3.0 3D Printer

The major printing parameters assessed are tabulated in Table 1. The infill density was set to 25% to avoid solid structures. The melting point of PLA and printing temperature at the nozzle is set accordance 215^0C.

Table 1: Printing parameters used to develop types of solar e-hubs.

Parameters	Values
Infill density	25%
Layer height	0.1 mm
Print speed	50 mms^{-1}
Final printing temperature	210^0 C
Initial printing temperature	210^0 C
Support pattern	Line
Support structure	Tree
Bed Temperature	55^0 C

Despite the promising capabilities of 3D printing modules, this study encountered several failures. Figure 6(a-c) illustrates a sample fabrication failure attributed to multiple factors. These include insufficient adhesive application on the printing bed, which compromised the bond between the model and the bed. Additionally, instability in the printing bed due to vibrations was observed. Furthermore, inaccuracies in the Z-axis calibration of the printer resulted in thin, disjointed slices rather than a cohesive structure. In Figure 6(a), irregular protrusions are evident, stemming

from dysfunction in the stepper motor. Poor layer adhesion contributed to weak connections between layers, manifesting in an uneven, spiked surface appearance.

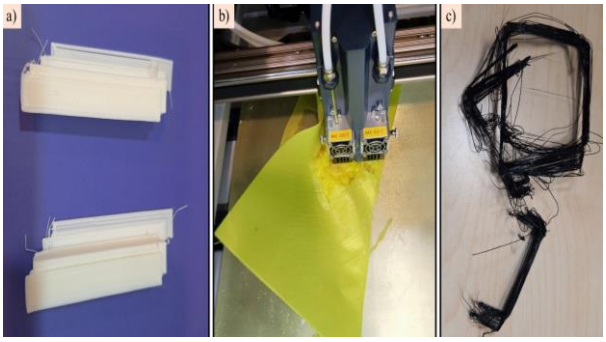

Figure 6. Failure printed samples

3.1 Solar module integration

Lab-scale solar cells were assembled with 3D fabricated solar e-hubs illustrated in Figures 7(a-c). Various 5V solar cells were mounted on the top surface. Inside the e-hubs, an IoT circuit featuring a 4-layer PCB, a 5V lithium-ion battery, and DHT22 temperature and humidity sensors operating at 5.5V were installed, as shown in Figure 7(d).

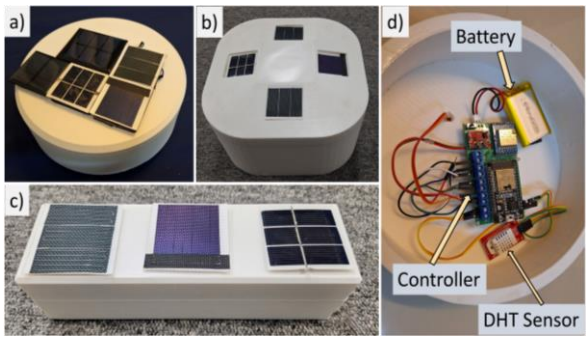

Figure 7. Solar module integrated different shaped solar ehubs; (a) circular, (b) cuboid, and (c) rectangular and d) integrated circuit of 1Watt

4. Mechanical characterization and discussion

The specimen geometry was created according to ASTM D695 standard [28] to analysis the mechanical behaviours of PLA materials by analysing FEA analysis, impact test, deformation test and hardness test.

4.1 Impact Test

The Charpy impact test was performed as per as the standard ASTM D6110 [29]. The impact test is a standardized testing method used to evaluate the ability of materials to withstand sudden loads or impacts. It involves subjecting the material to a controlled force or impact and measuring the energy absorbed or the damage caused by the impact. Five identical samples underwent impact testing to assess the properties of PLA material. These samples were modelled using Creo Parametric software, featuring dimensions of, impact specimen is square (12×12 mm^2) and 65 mm in length .. Fabrication was conducted using the 3D printer, utilizing PLA material. This samples were used to conduct the impact test, deformation test and hardness test. The ZwickRoell HIT50P machine was employed for conducting the impact tests and Charpy method was employed with 141^0 pendulum angle. The impact energy was recorded directly from the readout of impact tester. Figure 8 (a) shows the CAD model, Figure 8(b) shows 3D printed model, Figure 8(c-d) shows Charpy impact test machine and 8(e) shows specimen results after the testing. The obtained results of the impact tests are tabulated in the Table 2.

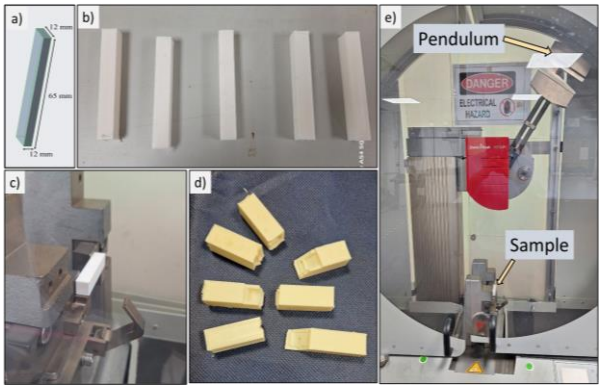

Figure 8. a) CAD model of impact test, b) 3D printed model, c) Impact Test Machine, d) Sample placed inside machine and e) Sampe results after the testing

The impact strength of the specimen was calculated using this following equation,

$$Impact\ Strength(I) = \frac{Impact\ Energy(K)}{Area(A)} \quad (1)$$

Where, K is the impact energy, A is the area of the specimen, and I is the impact strength. This analysis allows to understand the PLA material to resist cracking, and deformation under sudden and intense impact.

Table 2: Tabulated results of impact test analysis

Specimen	Material	Pendulum Energy (Joule)	Area (mm^2)	Impact Energy (Joule)	Impact Strength (Joule/ mm^2)	Angle of inclination (Degree)
1				4.78	0.03319	119.61
2				3.92	0.02722	123.93
3	PLA	25	144	3.43	0.02381	126.45
4				3.28	0.02277	127.26
5				2.99	0.02076	128.79

The impact strength results of the PLA samples were obtained by measuring the energy absorbed during the impact test. Equation 1 was used to determine the impact strength of the material. The results of the impact test showed that Sample 1 had the highest impact strength, absorbing a significant amount of energy before failure. On the other hand, Sample 2 exhibited a lower impact strength, indicating that it was more susceptible to failure under sudden loads. The relationship of the angle of contact during the impact test and the resulting impact strength is an important factor to consider. The results exhibit variations due to defects that occurred during fabrication, which were caused by fluctuating and unstable machine performance. As well as due to variations in pendulum velocity and the stricking point where the pendulum strikes the on sample. This slight variation in sample placement, that affects force distribution during impact test. These defects have a considerable effect on the impact test. The angle of contact can affect how the force is distributed over the material's surface during the impact, influencing the energy absorption and potential damage. Understanding the relationship between the angle of contact and impact strength can provide valuable insights into the material's performance under real-world impact scenarios [30].

4.2 Compression test

The standard ASTM D695 [28] compression test for rigid plastic was carried out in the study of PLA materials, ZwickRoell Z100 compression machine was used for implementing the test. The Figure 9 shows deformation test of PLA material. Stress and deformation analysis was performed to understand strength, elasticity, yield point, plasticity, and elongation during load. The Figure 10 shows the relationship between stress against deformation.

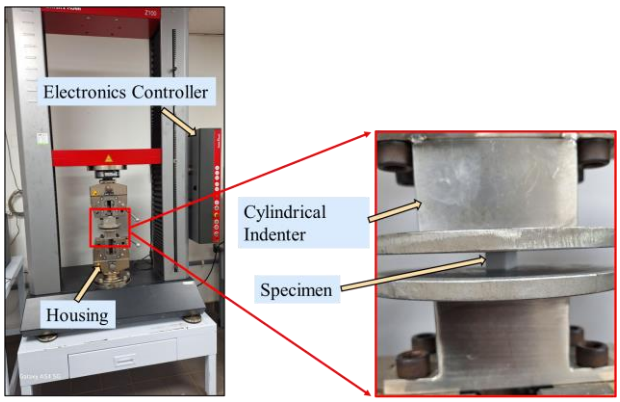

Figure 9. Deformation testing of PLA material specimen

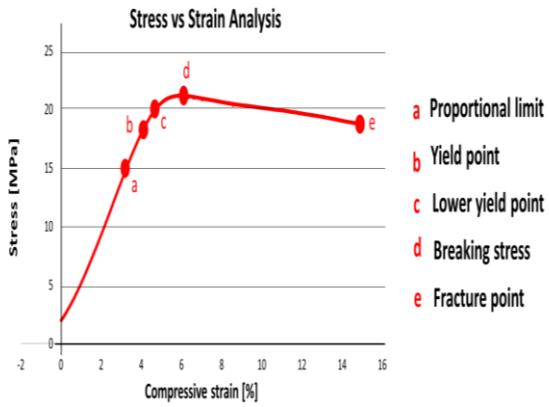

Figure 10. Stress and deformation study

Initially, deformation increased linearly with stress up to 15 MPa at region a, following a straight-line trend. The point OA in the graph represents the proportional limit. In this region the curve obeys Hooke's law. However, within the range of 15-20 MPa at region a, b-c, the material began to exhibit gradual signs of breakage as it surpassed the elastic region. Beyond this boundary, the material does not restore to its previous position, and a plastic deformation begins to occur in it. Beyond 20 MPa at region d, the linear relationship between stress and deformation ceased, with deformation failing to increase proportionally as stress continued to rise, leading to specimen breakage. At region e, the fracture of the material occurred.

4.3 Hardness test

The Rockwell hardness test was performed as per as the standard ASTM D785-08[31]. The hardness test is a prominent technique employed to determine the resistance of a material to indentation or scratching. In the study of PLA, ZwickRoell hardness machine was used for the testing, and the average of the testing obtained was 83.1 HRF. The Figure 11 shows the hardness results of PLA. The obtained results are tabulated in Table 3.

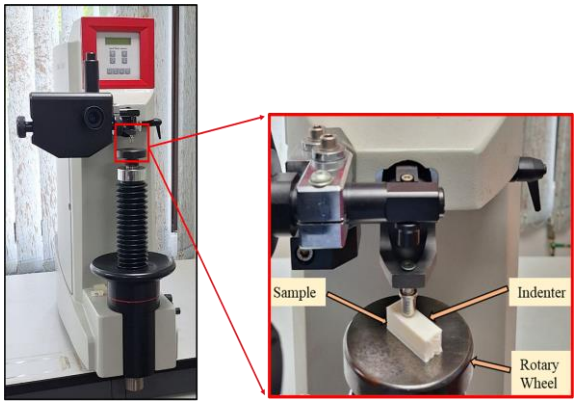

Figure 11. Hardness testing of PLA specimen

Table 3: Tabulated results of hardness analysis

Specimen	Material	Hardness Test (HRF)	Average Hardness (HRF)
1	PLA	83.2	83.1
2		82.5	
3		83.0	
4		83.5	
5		83.3	

This result indicates the level of hardness of the PLA material, suggesting its ability to resist indentation and scratching. The hardness of PLA is influenced by several factors for instances its molecular mass, crystallinity, density, and processing conditions. The indenter only touches the very top layer of the sample, making it generally less sensitive to microstructural variations and minor inconsistencies in the material. Since the test focuses on a small, localized area, it tends to produce consistent results across similar samples, especially in materials like PLA. Rockwell Hardness tests such as are designed for high precision and tend to have lesser variability as they are less affected by large-scale material inconsistencies. Additionally, the degree of crystallinity in PLA can also affect its hardness. Higher crystallinity tends to result in increased hardness [32].

In addition a visual aesthetical test has been performed by leaving one of the printed solar e-hubs in outdoor environment (Average weather conditions at UNITEN, Selangor, Malaysia, average temperature 35^0C and humidity 67-90% during the day time) continuously for 4 weeks to have a primary ideas on its structural and color stability. The figure 12 shows the images of solar e-hub before and after outdoor test.

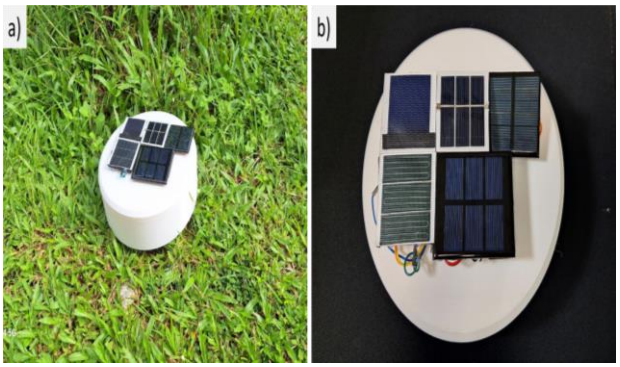

Figure 12. Images of solar e-hub a) before and, b) after outdoor test, no significance degradation (structural and visual) was observed

5. Future directions

This study emphasizes the significance of PLA material in advancing solar e-hub development, focusing on material selection, durability, and cost-effectiveness. PLA demonstrates excellent impact strength 4.8 Joules, a maximum load of 22 MPa, and a hardness of 83.1 HRF, making it suitable for solar e-hub applications. The integration of lab-scale solar cells, IoT circuits, Lithium-Ion batteries, and sensors within PLA-based solar hubs highlights practical applications, promoting sustainable energy solutions and the adoption of renewable energy technologies. However, several challenges and limitations that are inherent to the technology prints often exhibit visible layer lines and rough surface finishes, especially on curved or intricate geometries. Print success rates can vary depending on factors such as environmental conditions such as temperature, humidity and machine calibration. Inconsistent layer adhesion or nozzle clogging can lead to print failures and wasted material. FDM can generate significant waste material (e.g., support structures, failed prints) compared to other manufacturing methods. The integration of artificial intelligence in the current research can advancement the fabrication of solar e-hub. Integrating AI with FDM for rapid prototyping addresses its inherent limitations by optimizing print parameters to improve surface quality and reduce visible layer lines. Machine learning based applications in printing are crucial for achieving sustainable and efficient production, specifically in the perspective of PLA materials and 3D printing [33].

AI also improves quality control by automatically identifying printing defects, which allows for quick corrections for higher success rates. Through the process of standardization and less reliance on operator skill levels, AI enhances the dependability and efficiency of rapid prototyping using FDM technology. Real-time process control and print parameter optimization can be obtained by reinforcement learning (RL). Through interactions with the printing ambient, it allows the AI system to learn and adapt, changing temperature, speed, and layer height according to feedback it receives during the printing process. Figure 13 shows the RL functions as a learning model in machine learning to improve the FDM process in prototyping.

In order to enhance print quality and efficiency, RL for FDM 3D printing entails an agent modifying print parameters based on real-time feedback.

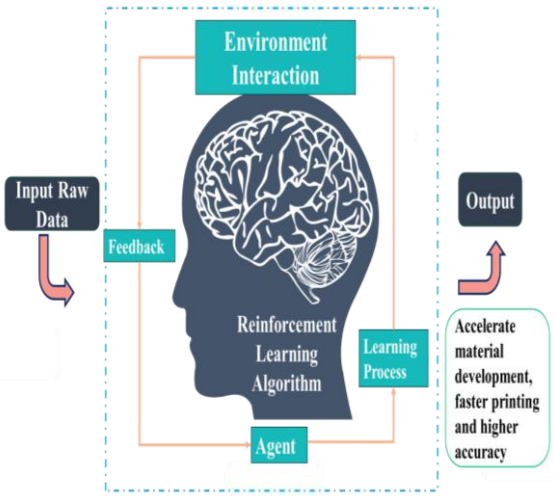

Figure 13. RL enhanced 3D printing

6. Conclusions

In conclusion, our comprehensive investigation involved the initial step of performing impact tests, compression test, and hardness testing on the PLA material. The results yielded favourable outcomes, affirming PLA's robustness and compatibility for use in solar e-hubs. The material exhibited a linear response to stress up to 15 MPa, beyond which signs of breakage began to manifest as it entered the plastic deformation region. Notably, PLA demonstrated resilience within this range, displaying its potential for withstanding moderate stress levels. Moreover, the hardness tests revealed PLA's ability to maintain structural integrity under various loading conditions. While our findings are promising, we acknowledge the importance of conducting environmental tests to comprehensively evaluate PLA's performance in real-world conditions. These tests will provide invaluable insights into the material's long-term durability and sustainability, ensuring its viability for prolonged use in solar e-hubs. The investigation has highlighted PLA as a viable and promising material choice for our project. Moving forward further research and testing to validate its performance under environmental stressors and optimize its utilization in solar e-hub applications. The flexibility in design offered by the FDM method allows for the creation of intricate and customized shapes that may not be feasible with traditional manufacturing methods.

Acknowledgment: The authors acknowledge the Ministry of Higher Education of Malaysia (MOHE) for the support given with the Higher Education Center of Excellence (HICoE) grant for this research with the grant code "JPT.S(BPKI)2000/016/018/015JId.4 (21) / 2022003HICOE" at the Innovation & Research Management Center (iRMC) of Universiti Tenaga Nasional (@UNITEN, The National Energy University), Malaysia.

References

[1] I. Fekete, F. Ronkay, and L. Lendvai, "Highly toughened blends of poly(lactic acid) (PLA) and natural rubber (NR) for FDM-based 3D printing applications: The effect of composition and infill pattern," *Polym. Test.*, vol. 99, 2021.

[2] A. Manmadhachary, "CT imaging parameters for precision models using additive manufacturing," *Multiscale Multidiscip. Model. Exp. Des.*, vol. 2, no. 3, pp. 209–220, 2019.

[3] T. DebRoy *et al.*, "Additive manufacturing of metallic components – Process, structure and properties," *Prog. Mater. Sci.*, vol. 92, pp. 112–224, 2018.

[4] G. Sharma, J. Sai, M. Kumar, S. Kumar, A. Anitha, and V. Kanwar, "Materials Today : Proceedings PLA material based development and advancement of low cost 3D printer using Fused Deposition Method," *Mater. Today Proc.*, no. July 2023, pp. 1–8, 2024.

[5] C. L. Gnanasagaran *et al.*, "Microstructural and mechanical behaviours of Y-TZP prepared via slip-casting and fused deposition modelling (FDM)," *Heliyon*, vol. 9, no. 11, p. e21705, 2023.

[6] N. Mohan, P. Senthil, S. Vinodh, and N. Jayanth, "A review on composite materials and process parameters optimisation for the fused deposition modelling process," *Virtual Phys. Prototyp.*, vol. 12, no. 1, pp. 47–59, 2017.

[7] A. G. Olabi and M. A. Abdelkareem, "Renewable energy and climate change," *Renew. Sustain. Energy Rev.*, vol. 158, p. 112111, Apr. 2022..

[8] J. Charles Rajesh Kumar and M. A. Majid, "Renewable energy for sustainable development in India: Current status, future prospects, challenges, employment, and investment opportunities," *Energy. Sustain. Soc.*, vol. 10, no. 1, pp. 1–36, Jan. 2020.

[9] S. Prathiba, A. Sheela, and S. Revathi, "Design and development of portable stand-alone solar power generator," *J. Green Eng.*, vol. 10, no. 6, pp. 2946–2955, 2020.

[10] M. S. Roslan, F. Adan, M. A. Mohammad, N. Norazman, S. Haizam, and Z. Haider, "Development of portable solar storage device," *J. Phys. Conf. Ser.*, vol. 1371, no. 1, 2019, doi: 10.1088/1742-6596/1371/1/012002.

[11] A. A. Badran, I. A. Yousef, N. K. Joudeh, R. Al Hamad, H. Halawa, and H. K. Hassouneh, "Portable solar cooker and water heater," *Energy Convers. Manag.*, vol. 51, no. 8, pp. 1605–1609, 2010.

[12] M. Nasir, A. R. Jordehi, M. Tostado-Véliz, V. S. Tabar, S. Amir Mansouri, and F. Jurado, "Operation of energy hubs with storage systems, solar, wind and biomass units connected to demand response aggregators," *Sustain. Cities Soc.*, vol. 83, p. 103974, Aug. 2022.

[13] P. Ortega-Arriaga, O. Babacan, J. Nelson, and A. Gambhir, "Grid versus off-grid electricity access options: A review on the economic and

environmental impacts," *Renew. Sustain. Energy Rev.*, vol. 143, p. 110864, Jun. 2021.

[14] A. T. de Almeida, P. Moura, and N. Quaresma, "Off-Grid Sustainable Energy Systems for Rural Electrification," pp. 1–22, 2020.

[15] M. Nur-E-Alam *et al.*, "Machine learning-enhanced all-photovoltaic blended systems for energy-efficient sustainable buildings," *Sustain. Energy Technol. Assessments*, vol. 62, no. November 2023, p. 103636, 2024.

[16] I. Iftekharuzzaman, S. Ghosh, M. K. Basher, M. A. Islam, N. Das, and M. Nur-E-Alam, "Design and Concept of Renewable Energy Driven Auto-Detectable Railway Level Crossing Systems in Bangladesh," *Futur. Transp.*, vol. 3, no. 1, pp. 75–91, 2023.

[17] B. F. Giannetti *et al.*, "Insights on the United Nations Sustainable Development Goals scope: Are they aligned with a 'strong' sustainable development?," *J. Clean. Prod.*, vol. 252, p. 119574, 2020.

[18] A. Selema *et al.*, "Material Engineering of 3D-Printed Silicon Steel Alloys for the Next Generation of Electrical Machines and Sustainable Electromobility," *J. Magn. Magn. Mater.*, vol. 584, no. August, p. 171106, 2023.

[19] T. Yao, Z. Deng, K. Zhang, and S. Li, "A method to predict the ultimate tensile strength of 3D printing polylactic acid (PLA) materials with di ff erent printing orientations," *Compos. Part B*, vol. 163, no. July 2018, pp. 393–402, 2019.

[20] N. A. A. B. Taib *et al.*, "A review on poly lactic acid (PLA) as a biodegradable polymer," *Polym. Bull.*, vol. 80, no. 2, pp. 1179–1213, Feb. 2023.

[21] G. Rajeshkumar *et al.*, "Environment friendly, renewable and sustainable poly lactic acid (PLA) based natural fiber reinforced composites – A comprehensive review," *J. Clean. Prod.*, vol. 310, p. 127483, Aug. 2021.

[22] L. Li, Q. Sun, C. Bellehumeur, and P. Gu, "Composite modeling and analysis for fabrication of FDM prototypes with locally controlled properties," *J. Manuf. Process.*, vol. 4, no. 2, pp. 129–141, 2002.

[23] G. W. Melenka, B. K. O. Cheung, J. S. Schofield, M. R. Dawson, and J. P. Carey, "Evaluation and prediction of the tensile properties of continuous fiber-reinforced 3D printed structures," *Compos. Struct.*, vol. 153, pp. 866–875, 2016.

[24] T. D. Ngo, A. Kashani, G. Imbalzano, K. T. Q. Nguyen, and D. Hui, "Additive manufacturing (3D printing): A review of materials, methods, applications and challenges," *Compos. Part B Eng.*, vol. 143, no. December 2017, pp. 172–196, 2018.

[25] O. A. Mohamed, S. H. Masood, and J. L. Bhowmik, "Optimization of fused deposition modeling process parameters: a review of current research and future prospects," *Adv. Manuf.*, vol. 3, no. 1, pp. 42–53, 2015.

[26] T. D. Ngo, A. Kashani, G. Imbalzano, K. T. Q. Nguyen, and D. Hui, "Additive manufacturing (3D printing): A review of materials, methods, applications and challenges," Compos. Part B Eng., vol. 143, no. December 2017, pp. 172–196, 2018.

[27] O. A. Mohamed, S. H. Masood, and J. L. Bhowmik, "Optimization of fused deposition modeling process parameters: a review of current research and future prospects," Adv. Manuf., vol. 3, no. 1, pp. 42–53, 2015.

[28] "Compression Testing: Machine & Test | Strength & Tension | ZwickRoell." https://www.zwickroell.com/industries/materials-testing/compression-test/ (Accessed:2024-03-04).

[29] ISO 179 Charpy impact test plastics | ZwickRoell https://www.zwickroell.com/industries/plastics/thermoplastics-and-thermosetting-molding-materials/charpy-impact-strength-notched-impact-strength-iso-179-1-iso-179-2/ (Accessed: 2024-08-24).

[30] A. J. M. Al-Behadili and B. O. Bedaiwi, "Experimental and Numerical Measurement of the Impact Strength of Poly-lactic Acid through a Low-velocity Impact," IOP Conf. Ser. Mater. Sci. Eng., vol. 1094, no. 1, p. 012171, 2021.

[31] Hardness tests on plastics | ZwickRoell https://www.zwickroell.com/industries/plastics/thermoplastics-and-thermosetting-molding-materials/hardness-testing/ (Accessed: 2024-08-24).

[32] Y. Li et al., "Evaluation of thermal resistance and mechanical properties of injected molded stereocomplex of poly(l-lactic acid) and poly(d-lactic acid) with various molecular weights," Adv. Polym. Technol., vol. 37, no. 6, pp. 1674–1681, 2018.

[33] K. Guo, Z. Yang, C. H. Yu, and M. J. Buehler, "Artificial intelligence and machine learning in design of mechanical materials," Mater. Horizons, vol. 8, no. 4, pp. 1153–1172, 2021.